

# Обзор ArXiv: astro-ph, 20-24 марта 2017

От Сильченко О.К.

# Astro-ph: 1703.06889

Invited Review for Nature Astronomy

## Impact of supermassive black hole growth on star formation

Chris Harrison<sup>1,2\*</sup>

<sup>1</sup>European Southern Observatory, Karl-Schwarzschild-Str. 2, 85748 Garching b. München, Germany

<sup>2</sup>Centre for Extragalactic Astronomy, Durham University, South Road, Durham, DH1 3LE, U.K.

\*ESO Fellow; c.m.harrison@mail.com

---

### Abstract

Supermassive black holes are found at the centre of massive galaxies. During the growth of these black holes they light up to become visible as active galactic nuclei (AGN) and release extraordinary amounts of energy across the electromagnetic spectrum. This energy is widely believed to regulate the rate of star formation in the black holes' host galaxies via so-called "AGN feedback". However, the details of how and when this occurs remains uncertain from both an observational and theoretical perspective. I review some of the observational results and discuss possible observational signatures of the impact of super-massive black hole growth on star formation.

---

# Теоретикам для спасения иерархической концепции нужен AGN feedback для массивных галактик

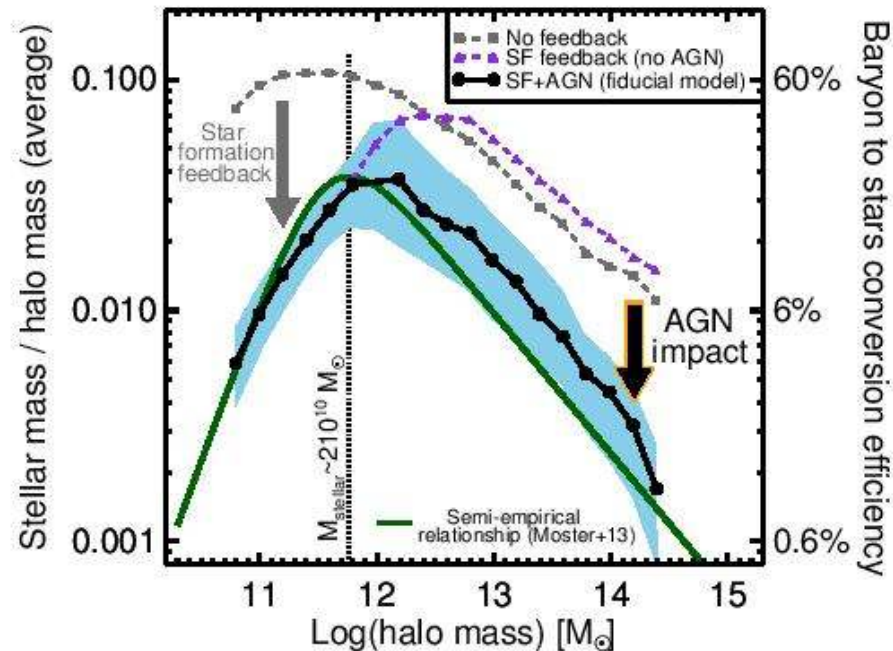
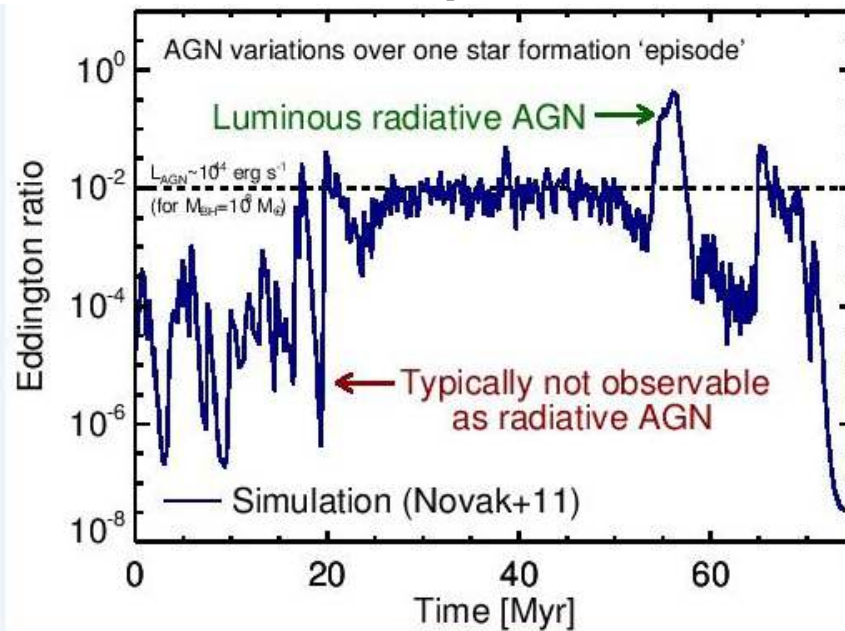


Figure 1 | The ratio of stellar mass to halo mass as a function of halo mass for three different runs of a simulation[6] and for the semi-empirical relationship[17]. The shaded region shows the 16th and 84th percentiles of the fiducial model that includes energy injection from AGN and star formation (SF). The right y-axis shows the efficiency for turning baryons into stars ( $M_{\text{stellar}}/[f_b * M_{\text{halo}}]$ ; where the factor of  $f_b = 0.17$  is the cosmological baryon fraction). The

# В моделях временная шкала AGN сильно короче временной шкалы звездообразования...



Box 2 | Eddington ratio versus times for an example simulation of an AGN to illustrate variability.

As discussed in detail in [98] various observational work indicates that AGN luminosities ( $L_{\text{AGN}}$ ), in particular those derived from optical and/or X-ray continuum measurements that trace effectively *instantaneous* mass accretion rates, vary on orders of magnitude on times scales much shorter than the typical timescale of star formation episodes ( $\gtrsim 100$  Myrs). Similar results are reached by AGN simulations; for example, the figure presents the results of the Eddington Ratio (proportional to the mass accretion rate and AGN luminosity) as a function of

- ПОЭТОМУ ТО, ЧТО НИКАКОГО FEEDBACK от AGN НЕ ВИДНО В НАБЛЮДЕНИЯХ – СОВСЕМ НЕ ЗНАЧИТ, ЧТО ЕГО НЕТ!

# Демонстрация этого тезиса

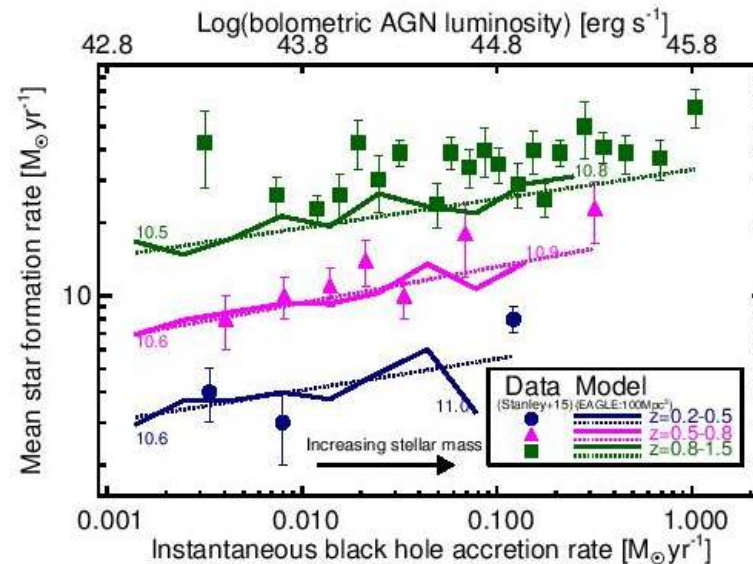


Figure 3 | Mean star formation rate versus instantaneous black hole accretion rate for a cosmological simulation[81] and versus AGN luminosity (converted from X-ray luminosities) for observations[79]. The dotted lines are a linear fit to the running means for the model (solid curves). The logarithm of the average 30 kpc aperture stellar masses (in stellar mass units) of the first and last bin are labelled; the slight increase in mean star-formation rate with increasing accretion rate is attributed to the increasing average stellar masses. Despite effective star-formation suppression by AGN in the model, this does not result in reduced average star-formation rates for the highest instantaneous black hole accretion

# А вот загиб «главной последовательности» на больших массах как раз вдохновляет!

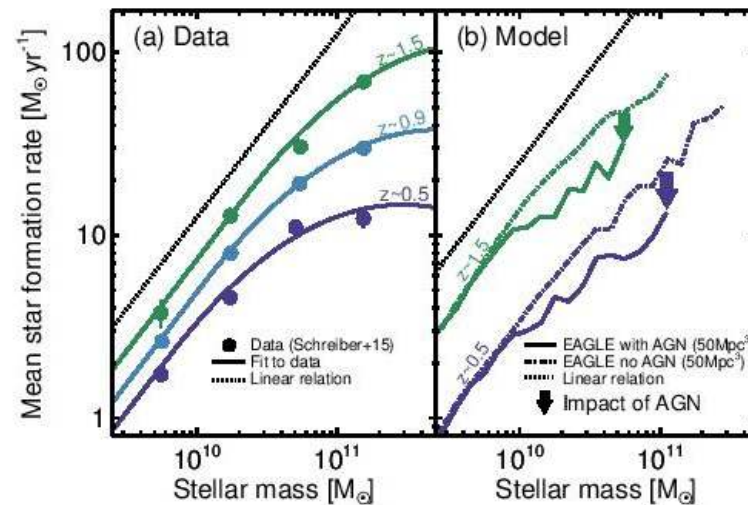


Figure 4 | Mean star formation rate versus stellar mass for observed star-forming galaxies[90] (a) and galaxies in a cosmological model run both with and without AGN[82, 11] (b). More massive galaxies form stars more rapidly; however, the highest-mass galaxies ( $M_{\text{stellar}} \gtrsim 10^{10} M_{\odot}$ ) are observed to fall below a constant scaling relationship implying a reduction in the ability for the available baryons to be converted into stars[89, 90]. In the model, the impact of AGN is to reduce star formation rates of high mass galaxies as well as to reduce the overall number of massive galaxies. Note that error bars are smaller than the data points in most cases[90].

- ОТ ЧЕГО БЫ ЕМУ БЫТЬ, КАК НЕ ОТ ФИД\_БЭКА?!



# Astro-ph: 1703.07365

Mon. Not. R. Astron. Soc. **000**, 1–9 (2017)      Printed 23 March 2017      (MN L<sup>A</sup>T<sub>E</sub>X style file v2.2)

## A detection of wobbling Brightest Cluster Galaxies within massive galaxy clusters

David Harvey<sup>1\*</sup>, F. Courbin<sup>1</sup>, J. P. Kneib<sup>1,2</sup>, Ian G. McCarthy<sup>3</sup>

<sup>1</sup>*Institute of Physics, Laboratoire d'Astrophysique, EPFL, Observatoire de Sauverny, 1290 Versoix, Switzerland*

<sup>2</sup>*Aix Marseille Universit, CNRS, LAM (Laboratoire d'Astrophysique de Marseille) UMR 7326, 13388, Marseille, France*

<sup>3</sup>*Astrophysics Research Institute, Liverpool John Moores University, 146 Brownlow Hill, Liverpool L3 5RF*

# Если есть осцилляция центральной галактики относительно центра масс, вот так она проявляется в мгновенных позиционных измерениях

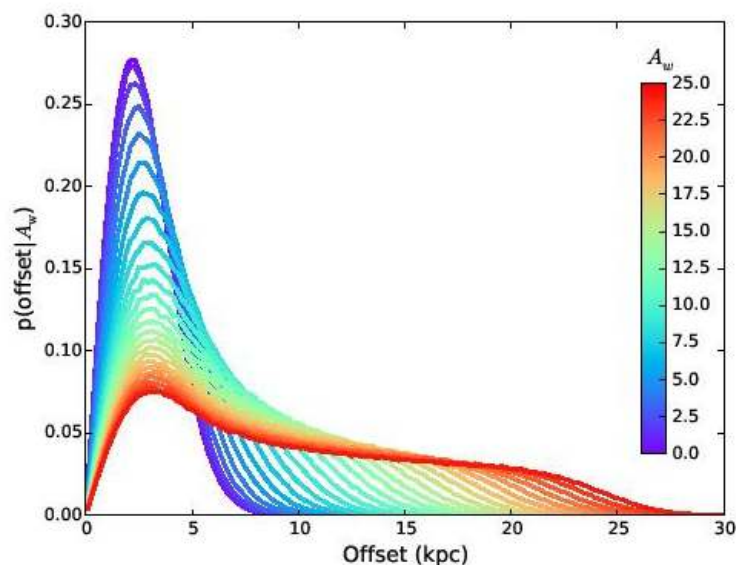


**Figure 2.** We calculate  $p(\text{offset}|A_w)$ , the expected posterior for the radial offset between BCG and cluster halo, given some wobble amplitude,  $A_w$  kpc. To do this we generate them numerically folding in the true redshift distributions of the clusters (see text). The kink in the tail of the posterior is due to the hard cut off in the simple harmonic oscillation convolved with statistical errors in position.

# Симуляции (статистика скоплений на $z < 0.25$ ) = VANAMAS, а наблюдательная выборка – вот она

Cluster	RA	DEC	$z$	$\Gamma$	$N_I$	$N_P$	RMS	$\delta_x$ (")	$\delta_y$ (")	$M_{200} (\times 10^{14} M_{\odot})$	$c_{200}$
A1063	342.18324	-44.53087	0.35	0.24	41	17	0.79	$0.05 \pm 0.12$	$-0.01 \pm 0.10$	$16.2 \pm 0.3$	$4.7 \pm 0.1$
A383	42.01409	-3.52938	0.19	0.53	26	11	0.55	$0.13 \pm 0.18$	$0.68 \pm 0.15$	$16.6 \pm 5.1$	$4.0 \pm 1.4$
A2261	260.61341	32.13266	0.22	0.36	32	20	0.52	$0.67 \pm 0.04$	$-0.56 \pm 0.05$	$6.9 \pm 0.6$	$9.0 \pm 0.5$
A1703	198.77197	51.81749	0.28	0.20	42	22	0.49	$-0.55 \pm 0.09$	$1.07 \pm 0.16$	$13.5 \pm 0.9$	$4.6 \pm 0.2$
A1835	210.25865	2.87847	0.25	0.51	18	14	0.29	$4.25 \pm 0.06$	$-0.64 \pm 0.12$	$28.7 \pm 1.7$	$3.7 \pm 0.2$
A1413	178.82449	23.40445	0.14	0.33	11	9	1.17	$0.07 \pm 0.06$	$-0.71 \pm 0.13$	$6.7 \pm 0.9$	$7.2 \pm 0.5$
MACS0744	116.21999	39.45740	0.69	0.38	20	19	0.13	$-0.62 \pm 0.21$	$-0.42 \pm 0.61$	$9.9 \pm 1.4$	$4.7 \pm 0.8$
MACS1206	181.55060	-8.80093	0.44	0.28	35	13	1.09	$-1.36 \pm 0.07$	$-0.36 \pm 0.03$	$15.0 \pm 0.2$	$4.8 \pm 0.1$
MACS1720	260.06980	35.60731	0.39	0.44	17	13	0.81	$0.61 \pm 0.04$	$-1.64 \pm 0.05$	$9.8 \pm 0.7$	$5.2 \pm 0.3$
MACS1931	292.95683	-26.57584	0.35	0.55	23	10	0.87	$0.45 \pm 0.03$	$1.91 \pm 0.09$	$9.7 \pm 0.3$	$5.0 \pm 0.1$

**Table 2.** The survey sample of the ten dynamically relaxed galaxy clusters in which we aim to measure the offset between the BCG and large scale main halo. *Col 2:* Right Ascension, *Col 3:* Declination, *Col 4:* Cluster redshift, *Col 5:* Dynamical state (eq. (1)), *Col 6:* Number of multiple images, *Col 7:* Number of parameters in the fit *Col 8:* Root mean square error of the mode fit, *Col 9 & 10:* the offset between the BCG and the large scale halo in arc-seconds, *Col 11:* Mass of the cluster halo and *Col 12:* the concentration parameter. All uncertainties are purely statistical Gaussian errors as reported by LENSTOOL.

# Результат: в реальных скоплениях – не CDM

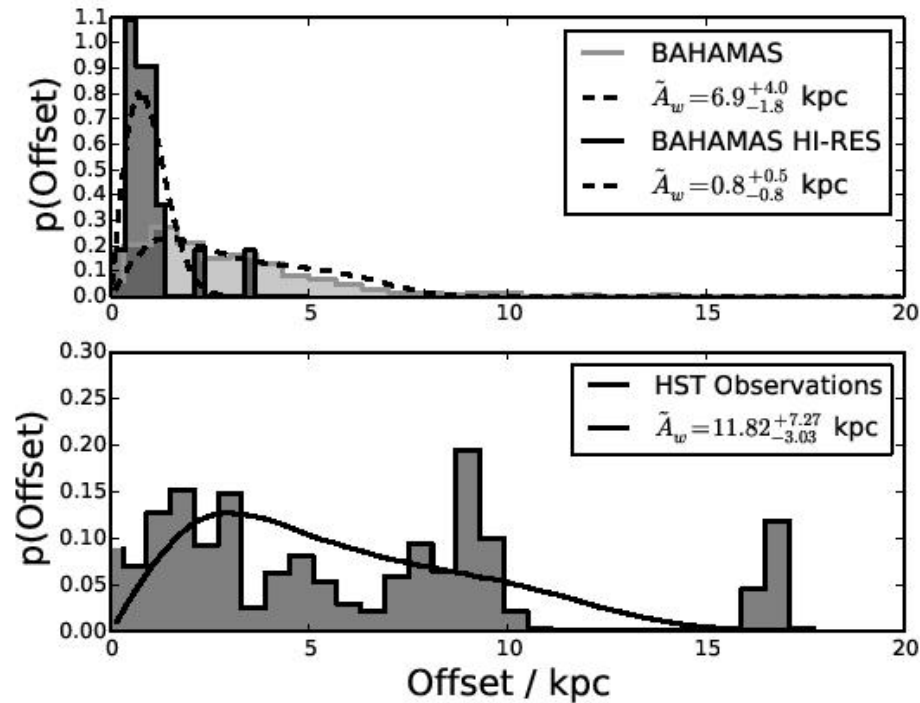


**Figure 4.** The top panel shows the distribution of radial offsets between the BCG and the dark matter potential in the BAHAMAS simulations. We analyse both the fiducial resolution sample consisting on 600 clusters, and the high resolution sample of 22 clusters. The dark histogram and associated dashed line represent the offsets in the high-resolution sample and its best fit to the numerical posteriors. The light-grey histogram and associated dashed line show the distribution of offsets in the high-resolution simulation and its best fit posterior. The legend shows the wobble amplitude for these best fit lines and their associated errors. The

# Astro-ph: 1703.07778

## KMOS<sup>3D</sup> REVEALS LOW-LEVEL STAR FORMATION ACTIVITY IN MASSIVE QUIESCENT GALAXIES AT $0.7 < z < 2.7$

SIRIO BELL<sup>1</sup>, REINHARD GENZEL<sup>1,2,3</sup>, NATASCHA M. FÖRSTER SCHREIBER<sup>1</sup>, EMILY WISNOSKI<sup>1</sup>, DAVID J. WILMAN<sup>1,5</sup>, STIJN WUYTS<sup>4</sup>, J. TREVOR MENDEL<sup>1</sup>, ALESSANDRA BEIFIORI<sup>1,5</sup>, RALF BENDER<sup>1,5</sup>, GABRIEL B. BRAMMER<sup>6</sup>, ANDREAS BURKERT<sup>1,5</sup>, JEFFREY CHAN<sup>1,5,7</sup>, REBECCA L. DAVIES<sup>1</sup>, RIC DAVIES<sup>1</sup>, MAXIMILIAN FABRICIUS<sup>1,5</sup>, MATTEO FOSSATI<sup>1</sup>, AUDREY GALAMETZ<sup>1</sup>, PHILIPP LANG<sup>1</sup>, DIETER LUTZ<sup>1</sup>, IVELINA G. MOMCHEVA<sup>6</sup>, ERICA J. NELSON<sup>1</sup>, ROBERTO P. SAGLIA<sup>1,5</sup>, LINDA J. TACCONI<sup>1</sup>, KEN-ICHI TADAKI<sup>1</sup>, HANNAH ÜBLER<sup>1</sup>, PIETER VAN DOKKUM<sup>8</sup>,

### ABSTRACT

We explore the H $\alpha$  emission in the massive quiescent galaxies observed by the KMOS<sup>3D</sup> survey at  $0.7 < z < 2.7$ . The H $\alpha$  line is robustly detected in 20 out of 120 *UVJ*-selected quiescent galaxies, and we classify the emission mechanism using the H $\alpha$  line width and the [N II]/H $\alpha$  line ratio. We find that AGN are likely to be responsible for the line emission in more than half of the cases. We also find robust evidence for star formation activity in nine quiescent galaxies, which we explore in detail. The H $\alpha$  kinematics reveal rotating disks in five of the nine galaxies. The dust-corrected H $\alpha$  star formation rates are low ( $0.2 - 7 M_{\odot}/\text{yr}$ ), and place these systems significantly below the main sequence. The  $24\mu\text{m}$ -based infrared luminosities, instead, overestimate the star formation rates. These galaxies present a lower gas-phase metallicity compared to star-forming objects with similar stellar mass, and many of them have close companions. We therefore conclude that the low-level star formation activity in these nine quiescent galaxies is likely to be fueled by inflowing gas or minor mergers, and could be a sign of rejuvenation events.

# Отобрали галактики без звездообразования ПО ЦВЕТУ

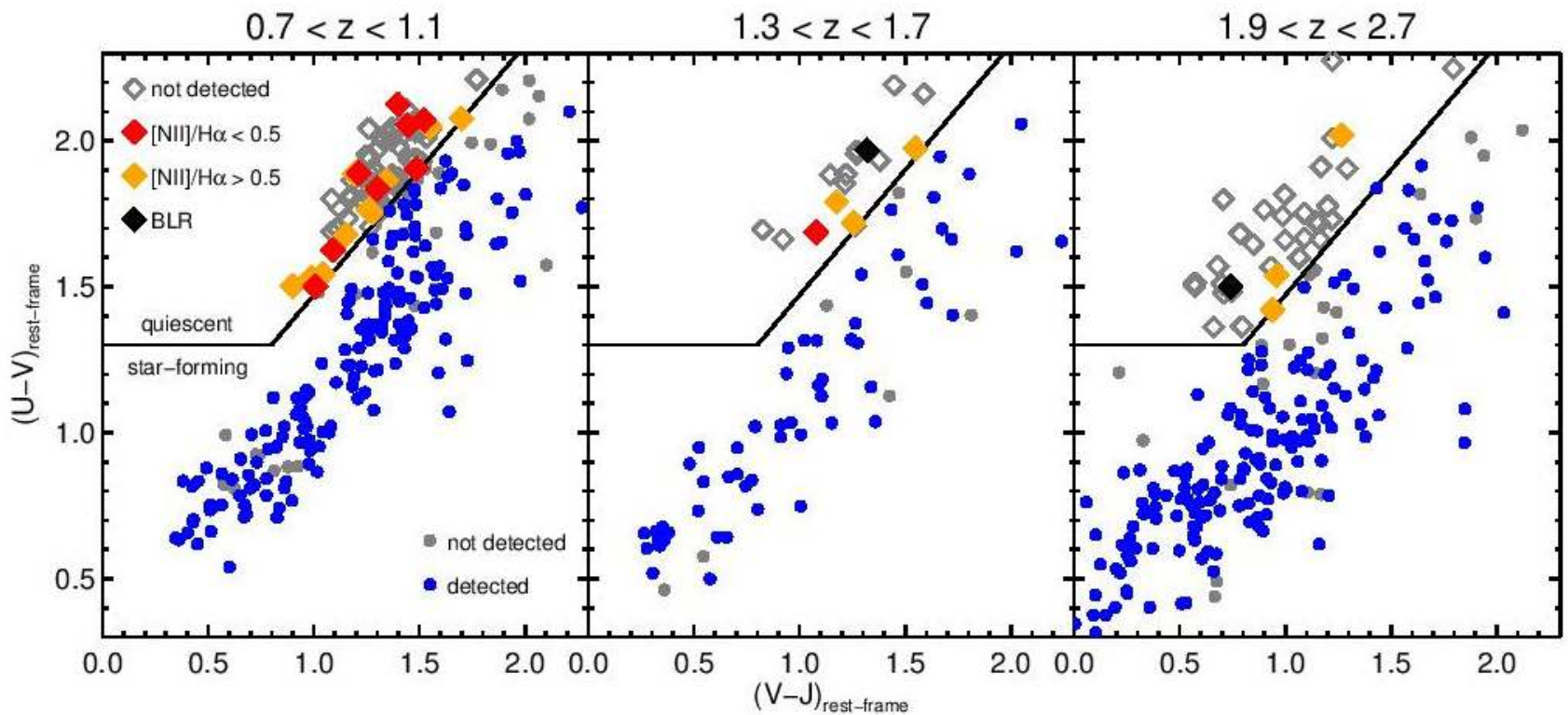
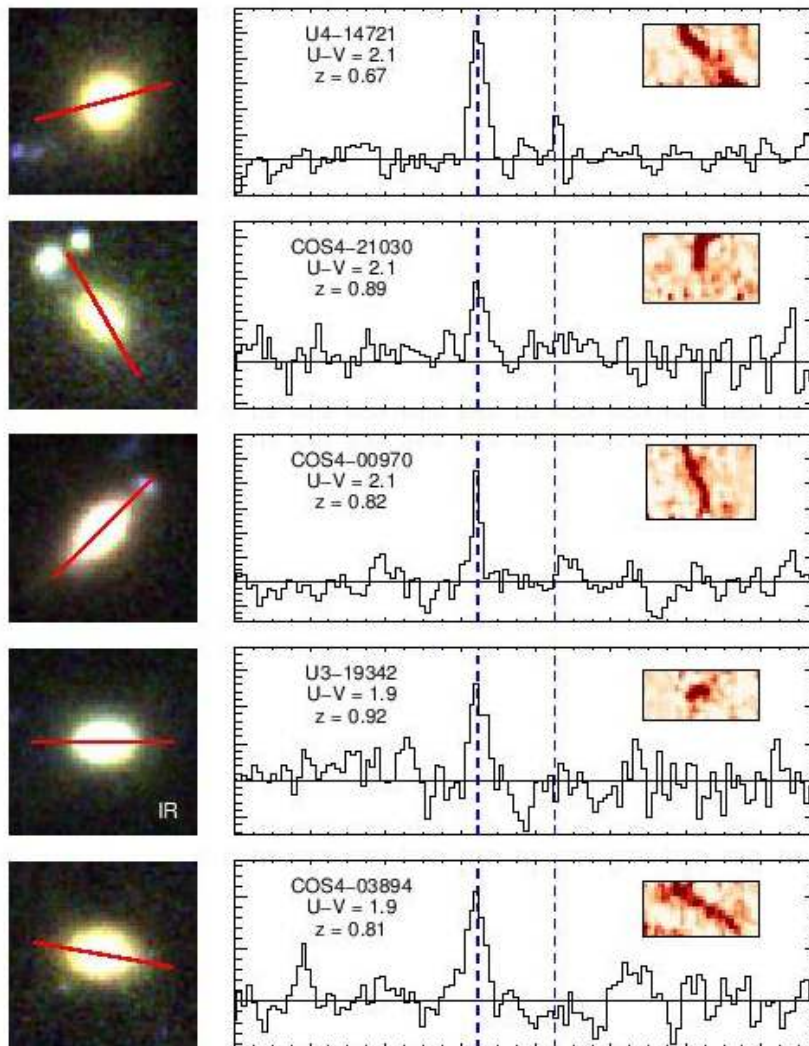


**Figure 1.**  $UVJ$  diagram for the KMOS<sup>3D</sup> sample, split into redshift bins. The solid line separates quiescent (diamonds) from star-forming galaxies (circles). Filled diamonds mark quiescent galaxies detected in  $H\alpha$ , with colors indicating the type of emission. Star-forming galaxies detected in  $H\alpha$  are shown in blue.

А в них протяженная H-alpha  
сильнее азота минимум в 2 раза!



# Это звездообразование, но с пониженной эффективностью

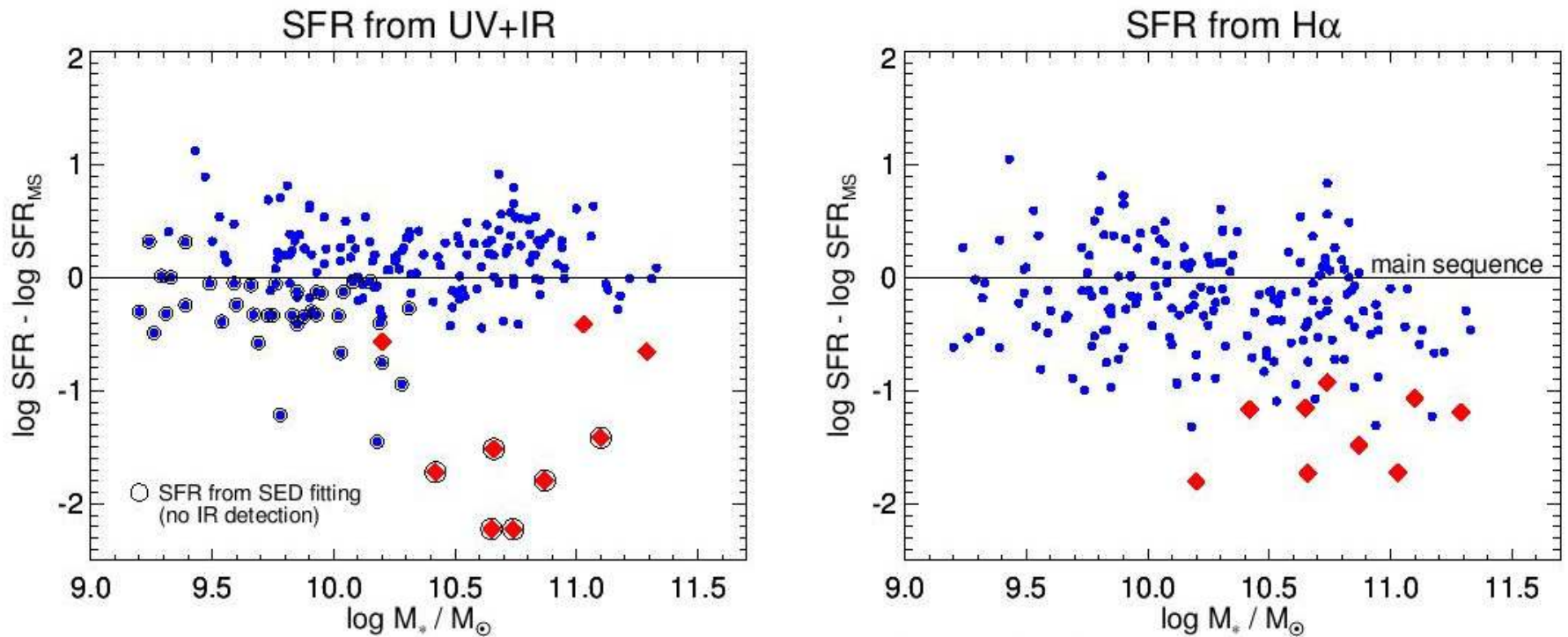


**Figure 5.** Vertical distance from the main sequence (as given by [Whitaker et al. 2014](#)), in logarithmic units, as a function of stellar mass. Star formation rates are derived from UV+IR luminosities (left panel) and dust-corrected H $\alpha$  fluxes (right panel). Symbols and colors as in Figure 1; only galaxies at  $z < 1.7$  and with  $[\text{N II}]/\text{H}\alpha < 0.5$  are shown.